Data in brief 28 (2020) 104922

Contents lists available at ScienceDirect

Data in brief

journal homepage: www.elsevier.com/locate/dib

Data Article

Kinetic data analysis of chaperone-like activity of Wt, R69C and D109H αB-crystallins

Maryam Ghahramani [a], Reza Yousefi [a, *], Alexey Krivandin [b], Konstantin Muranov [b], Boris Kurganov [c], Ali Akbar Moosavi-Movahedi [d]

[a] Protein Chemistry Laboratory (PCL), Department of Biology, College of Sciences, Shiraz University, Shiraz, Iran
[b] Emanuel Institute of Biochemical Physics, Russian Academy of Sciences, Kosygin str. 4, Moscow 119991, Russia
[c] Bach Institute of Biochemistry, Research Center of Biotechnology of the Russian Academy of Sciences, 33, bld. 2 Leninsky Ave., Moscow 119071, Russia
[d] Institute of Biochemistry and Biophysics (IBB), University of Tehran, Tehran, Iran

ARTICLE INFO

Article history:
Received 13 November 2019
Received in revised form 25 November 2019
Accepted 27 November 2019
Available online 4 December 2019

Keywords:
Human αB-crystallin
Chaperone-like activity
Kinetic data
Aggregation
Light scattering

ABSTRACT

The α-Crystallin (α-Cry) functions as a molecular chaperone, preventing the formation of stress-induced protein aggregation which is important for maintenance of lens transparency. The kinetic data of Wt, R69C and D109H αB-Crys chaperone-like activity were obtained by UV–Vis spectroscopy in both thermal- and chemical-induced aggregation methods. The data were analyzed using physical parameters describing the aggregation process including t^* (the characteristic of the stage of nucleation), and $t_{0.5}$ (the characteristic of the stage of aggregate growth) and I_{lim} (the limiting value of the light scattering intensity). Parameter t^* is duration of the lag phase and the lower t^* value is associated with the higher rate of the nucleation stage. Also, the lower values of $t_{0.5}$ indicated the higher rate of aggregate growth stage. The change in parameter I_{lim} in the presence of chaperones can be connected with the change in the size of protein aggregates. These data are related to the research article entitled "*Structural and functional characterization of D109H and R69C mutant versions of human*

DOI of original article: https://doi.org/10.1016/j.ijbiomac.2019.09.239.
* Corresponding author.
E-mail address: ryousefi@shirazu.ac.ir (R. Yousefi).

https://doi.org/10.1016/j.dib.2019.104922

αB-crystallin: the biochemical pathomechanism underlying cataract and myopathy development" [1].

Specifications Table

Subject	Biochemistry
Specific subject area	αB-crystallin, Chaperone-like activity, Aggregation
Type of data	Graphs and tables of kinetic data analyses
How data were acquired	Protein aggregation assessment by monitoring light scattering at 360 nm as a function of time, using a T90$^+$ UV–Vis spectrophotometer (PG Instrument Ltd., UK) equipped with a Peltier temperature controller.
Data format	Raw and analyzed
Parameters for data collection	Chaperone-like activity of Wt, R69C and D109H αB-Crys was evaluated with different client proteins including: insulin, lysozyme, catalase and γ-Cry, in both thermal- and chemical-induced aggregation methods.
Description of data collection	Aggregation of different client proteins in the absence and presence of chaperones was assessed by monitoring light scattering at 360 nm as a function of time, using UV–Vis spectroscopy.
Data source location	Shiraz University, Shiraz, Iran
Data accessibility	With the article
Related research article	M. Ghahramani, R. Yousefi, A. Krivandin, K. Muranov, B. Kurganov, A.A. Moosavi-Movahedi, Structural and functional characterization of D109H and R69C mutant versions of human αB-crystallin: the biochemical pathomechanism underlying cataract and myopathy development, Int. J. Biol. Macromol. S0141-8130 (2019) 34809-3. doi: 10.1016/j.ijbiomac.2019.09.239.

Value of the Data

- The data provide a further mechanistic insight into anti-aggregation ability of human αB-Cry and its mutant forms (R69C and D109H).
- The data might be used for modulating chaperone activity of the mutant proteins using chemical chaperones.
- These data also show the effect of each chaperone on the important parameters shaping chaperoning activity.
- These data clearly display the client protein-specific chaperone activity of the mutant proteins.

1. Data

1.1. Kinetic data analysis of chaperone-like activity of different αB-Crys

The aggregation process, obeying the mechanism of nucleation-dependent aggregation, involves the stage of nucleation and the stage of aggregate growth. When studying the aggregation kinetics by registration of increment of the light scattering intensity, the following equation is often applicable for description of the dependence of the light scattering intensity on time [2–4]:

$$I = I_{\lim}\{1 - \exp[-k_I(t - t^*)]\}, (t > t^*) \quad (1)$$

where k_I is the rate constant of the first order, I, I_0 and $I_{\lim}$ are the current, initial (at $t = 0$) and limiting (at $t \to \infty$) values of the light scattering intensity and t^* is a point in time corresponding to crossing of the theoretical curve, which calculated with this equation, with the horizontal line $I = 0$ calculated with this equation. Parameter t^* is duration of the lag phase and may be considered as a characteristic of the rate of the nucleation stage. The lower the t^* value, the higher is the rate of the nucleation stage. Eq. (1) can be transformed as follows:

$$I = I_{\lim}\{1 - \exp[-(\ln 2)(t - t^*)/t_{0.5}]\} \quad (2)$$

($t_{0.5} = \ln 2/k_I$)

The physical sense of parameter $t_{0.5}$ is the following. At $t = (t^* + t_{0.5})$ the value of I is equal to $I_{\lim}/2$. Parameter $t_{0.5}$ may be considered as a characteristic of the rate of the stage of aggregate growth. The lower the $t_{0.5}$ value, the higher is the rate of the stage of aggregate growth. The change in parameter $I_{\lim}$ in the presence of chaperones can be connected with the change in the size of protein aggregates. The diminishing of the $I_{\lim}$ value in the presence of chaperones can be due to the decrease in the size of protein aggregates.

1.1.1. Aggregation of insulin in the presence of 20 mM DTT (42 °C)

Fig. 1A shows the kinetics of DTT-induced aggregation of insulin at 42 °C. The initial kinetic data are represented in Table S1 in supplementary materials [1]. As can be seen from this Figure, at rather high values of time the light scattering intensity increases linearly with increasing time. Taking into account

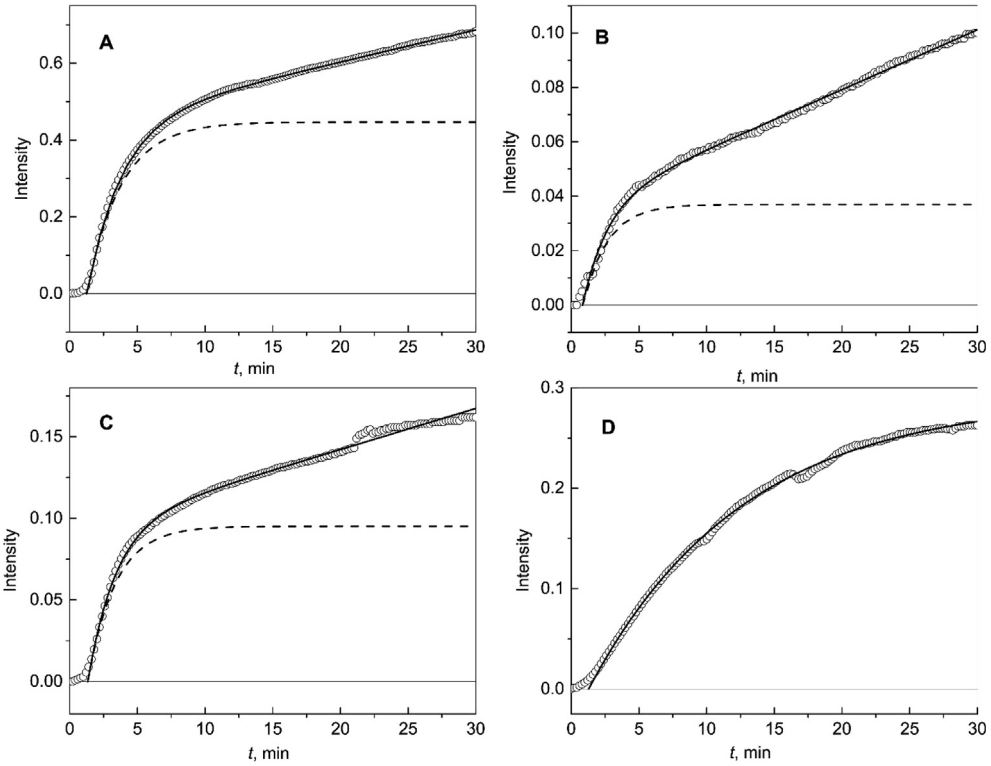

Fig. 1. Aggregation of insulin (0.3 mg mL^{-1}) in the presence of 20 mM DTT at 42 °C. (A) The dependence of the light scattering intensity (I) on time (t) for aggregation of insulin in the absence of any additives. Points are experimental data. Solid curve was calculated from Eq. (3) at the following values of parameters: $I_{\lim} = 0.447$, $t^* = 1.25$ min, $t_{0.5} = 1.76$ min and $B = 0.00834$ min^{-1}. Dotted curve was calculated from Eq. (2) at the following values of parameters: $I_{\lim} = 0.447$, $t^* = 1.25$ min and $t_{0.5} = 1.76$ min. (B) The dependence of I on t for aggregation of insulin in the presence of Wt αB-Cry (0.08 mg mL^{-1}). Solid curve was calculated from Eq. (3) at the following values of parameters: $I_{\lim} = 0.037$, $t^* = 0.84$ min, $t_{0.5} = 1.26$ min and $B = 0.00220$ min^{-1}. Dotted curve was calculated from Eq. (2) at the following values of parameters: $I_{\lim} = 0.037$, $t^* = 0.84$ min and $t_{0.5} = 1.26$ min. (C) The dependence of I on t for aggregation of insulin in the presence of R69C mutant form of αB-Cry (0.08 mg mL^{-1}). Solid curve was calculated from Eq. (3) at the following values of parameters: $I_{\lim} = 0.095$, $t^* = 1.33$ min, $t_{0.5} = 1.42$ min and $B = 0.00252$ min^{-1}. Dotted curve was calculated from Eq. (2) at the following values of parameters: $I_{\lim} = 0.095$, $t^* = 1.33$ min and $t_{0.5} = 1.42$ min. (D) The dependence of I on t for aggregation of insulin in the presence of D109H mutant form of αB-Cry (0.08 mg mL^{-1}). Solid curve was calculated from Eq. (2) at the following values of parameters: $I_{\lim} = 0.289$, $t^* = 1.28$ min, $t_{0.5} = 7.87$ min.

this peculiarity of the shape of the kinetic curve, the following equation can be proposed for description of the dependence of the light scattering intensity on time:

$$I = I_{\lim}\{1 - \exp[-(\ln 2)(t - t^*)/t_{0.5}]\} + B(t - t^*), \quad (3)$$

where B is constant. This equation was used to describe the kinetic curves of insulin aggregation in the absence of any additives (Fig. 1A, $B = 0.00834 \pm 0.00006$ min^{-1}) and in the presence of Wt αB-Cry (Fig. 1B; $B = 0.00220 \pm 0.00002$ min^{-1}) and in the presence of R69C mutant form of αB-Cry (Fig. 1C; $B = 0.00252 \pm 0.00004$ min^{-1}). When studying the effect of D109H mutant form of αB-Cry on insulin aggregation, Eq. (2) was used for description of the kinetic curve ($B = 0$). Parameters $I_{\lim}$, t^* and $t_{0.5}$ for insulin aggregation calculated using theoretical equations (2) and (3) are given in Table 1.

Table 1
Analyzed parameters for kinetic data on different client-protein aggregation.

Additives	$I_{\lim}$	t^*, min	$t_{0.5}$, min	m	R^2
DTT-induced aggregation of insulin at 42 °C					
No additives	0.447 ± 0.001	1.25 ± 0.01	1.76 ± 0.02	1	0.9994
αB-crystallin Wt	0.037 ± 0.001	0.84 ± 0.04	1.26 ± 0.05	1	0.9976
αB-crystallin R69C	0.095 ± 0.001	1.33 ± 0.04	1.42 ± 0.05	1	0.9953
αB-crystallin D109H	0.289 ± 0.001	1.28 ± 0.04	7.87 ± 0.09	1	0.9985
Aggregation of catalase at 60 °C					
No additives	1.06 ± 0.02	2.55 ± 0.02	3.42 ± 0.13	3.16 ± 0.11	0.9989
αB-crystallin Wt	0.110 ± 0.001	1.83 ± 0.02	3.65 ± 0.05	1.93 ± 0.06	0.9989
αB-crystallin R69C	0.0384 ± 0.0005	1.65 ± 0.02	1.67 ± 0.04	2.08 ± 0.10	0.9898
αB-crystallin D109H	0.600 ± 0.001	2.62 ± 0.01	3.04 ± 0.01	1.10 ± 0.01	0.9998
DTT-induced aggregation of lysozyme at 42 °C					
No additives	1.220 ± 0.007	8.34 ± 0.07	7.90 ± 0.07	1.18 ± 0.03	0.9991
αB-crystallin Wt	0.745 ± 0.003	27.7 ± 0.2	6.69 ± 0.15	0.69 ± 0.03	0.9978
αB-crystallin R69C	0.848 ± 0.001	18.0 ± 0.1	11.4 ± 0.1	0.55 ± 0.01	0.9997
αB-crystallin D109H	1.020 ± 0.007	22.2 ± 0.1	8.22 ± 0.06	1.02 ± 0.03	0.9996
Aggregation of γ-crystallin at 60 °C					
No additives	1.138 ± 0.002	9.5 ± 0.1	8.0 ± 0.1	0.75 ± 0.02	0.9987
αB-crystallin Wt	0.717 ± 0.002	20.8 ± 0.1	8.1 ± 0.1	0.69 ± 0.02	0.9988
αB-crystallin R69C	0.811 ± 0.001	21.0 ± 0.1	4.2 ± 0.1	0.85 ± 0.02	0.9978
αB-crystallin D109H	0.788 ± 0.002	15.8 ± 0.1	4.6 ± 0.1	1.03 ± 0.03	0.9976

1.1.2. Aggregation of catalase at 60 °C

Fig. 2A shows the kinetics of aggregation of catalase at 60 °C. The initial kinetic data are represented in Table S2 in supplementary materials. To analyze the shape of the kinetic curve, we have constructed the dependence of derivative dI/dt on I (Fig. 2B). The dependence of dI/dt on I can be described by equation [3]:

$$\frac{dI}{dt} = D(I_{\lim} - I)^m, \quad (4)$$

where D is constant. Parameter m was found to be equal to 3.4 ± 0.2.

Integration of Eq. (4) gives the following expression:

$$I = I_{\lim}\left\{1 - \frac{1}{\left[1 + \left(2^{m-1} - 1\right)(t - t^*)/t_{0.5}\right]^{1/(m-1)}}\right\}. \quad (5)$$

It should be noted, if $m = 1$, the dependence of the light scattering intensity on time follows Eq. (2).

Fig. 3 shows the kinetics of aggregation of catalase in the presence of Wt, R69C and D109H αB-Crys. Parameters $I_{\lim}$, t^*, $t_{0.5}$ and m calculated for the kinetic curves using Eq. (5) are given in Table 1.

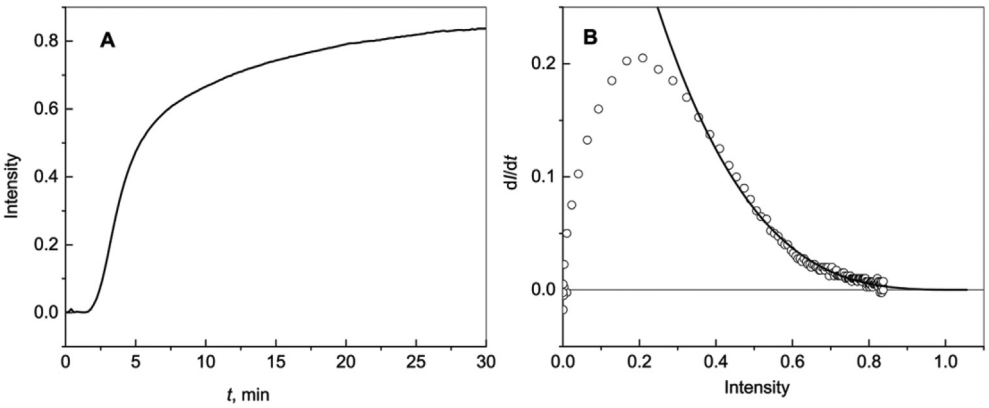

Fig. 2. Aggregation of catalase (0.3 mg mL^{-1}) at 60 °C. (A) The dependence of the light scattering intensity (I) on time (t). (B) The dependence of derivative dI/dt on the light scattering intensity. Points are experimental data. Solid curve was calculated from Eq. (4) at the following values of parameters: $D = 0.50$ min^{-1}, $I_{lim} = 1.06$ and $m = 3.4$.

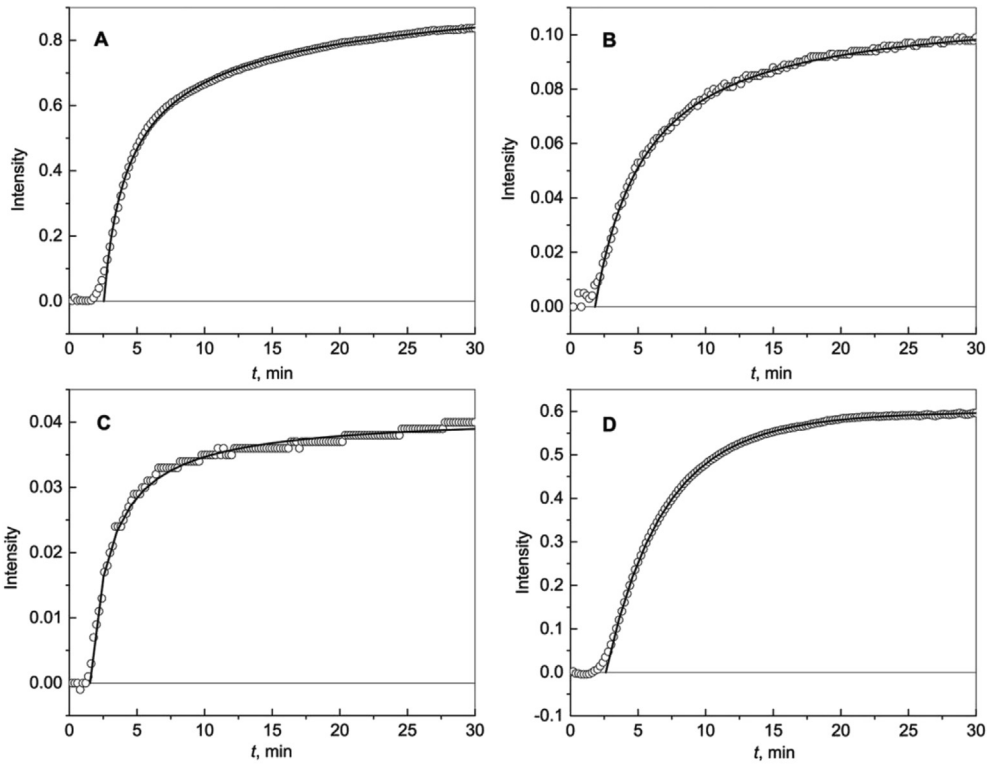

Fig. 3. Effect of αB-Cry and mutant forms of αB-Cry on aggregation of catalase (0.3 mg mL^{-1}) at 60 °C. (A) The dependence of the light scattering intensity (I) on time (t) for aggregation of catalase in the absence of any additives. Points are experimental data. Solid curve was calculated from Eq. (5) at the following values of parameters: $I_{lim} = 1.06$, $t^* = 2.55$ min, $t_{0.5} = 3.42$ min and $m = 3.2$. (B) The dependence of I on t for aggregation of catalase in the presence of Wt αB-Cry (0.08 mg mL^{-1}). Solid curve was calculated from Eq. (5) at the following values of parameters: $I_{lim} = 0.110$, $t^* = 1.83$ min, $t_{0.5} = 3.65$ min and $m = 1.93$. (C) The dependence of I on t for aggregation of catalase in the presence of R69C mutant form of αB-Cry (0.08 mg mL^{-1}). Solid curve was calculated from Eq. (5) at the following values of parameters: $I_{lim} = 0.0414$, $t^* = 1.53$ min, $t_{0.5} = 1.54$ min and $m = 2.1$. (D) The dependence of I on t for aggregation of catalase in the presence of D109H mutant form of αB-Cry (0.08 mg mL^{-1}). Solid curve was calculated from Eq. (5) at the following values of parameters: $I_{lim} = 0.600$, $t^* = 2.62$ min, $t_{0.5} = 3.04$ min and $m = 1.10$.

1.1.3. Aggregation of lysozyme in the presence of 20 mM DTT (42 °C)

Kinetics of DTT-induced aggregation of lysozyme at 42 °C in the absence and in the presence of Wt, R69C and D109H αB-Crys (Fig. 4) was analyzed using Eq. (5). The initial kinetic data are represented in Table S3 in supplementary materials. Parameters I_{lim}, t^*, $t_{0.5}$ and m for lysozyme aggregation are given in Table 1.

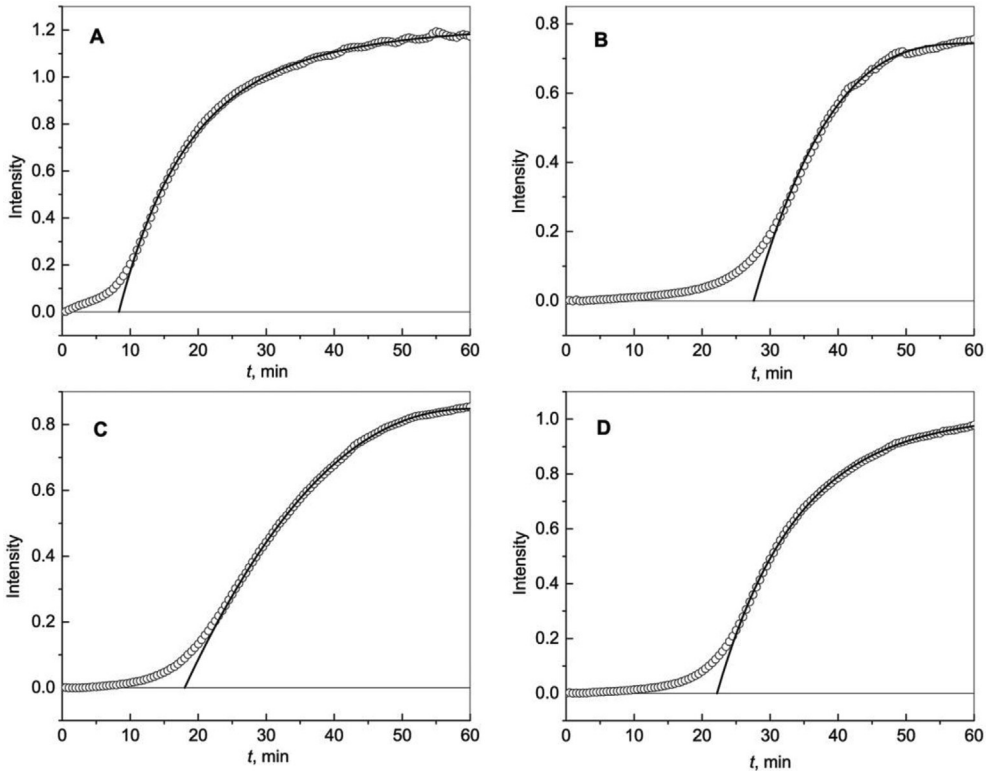

Fig. 4. Aggregation of lysozyme (0.2 mg mL^{-1}) in the presence of 20 mM DTT at 42 °C. (A) The dependence of the light scattering intensity (I) on time (t) for aggregation of lysozyme in the absence of any additives. Points are experimental data. Solid curve was calculated from Eq. (5) at the following values of parameters: I_{lim} = 1.220, t^* = 8.34 min, $t_{0.5}$ = 7.90 min and m = 1.18. (B) The dependence of I on t for aggregation of lysozyme in the presence of Wt αB-Cry (0.08 mg mL^{-1}). Solid curve was calculated from Eq. (5) at the following values of parameters: I_{lim} = 0.745, t^* = 27.7 min, $t_{0.5}$ = 6.69 min and m = 0.69. (C) The dependence of I on t for aggregation of lysozyme in the presence of R69C mutant form of αB-Cry (0.08 mg mL^{-1}). Solid curve was calculated from Eq. (5) at the following values of parameters: I_{lim} = 0.848, t^* = 18.0 min, $t_{0.5}$ = 11.4 min and m = 0.55. (D) The dependence of I on t for aggregation of lysozyme in the presence of D109H mutant form of αB-Cry (0.08 mg mL^{-1}). Solid curve was calculated from Eq. (2) at the following values of parameters: I_{lim} = 1.020, t^* = 22.2 min, $t_{0.5}$ = 8.22 min and m = 1.02.

1.1.4. Aggregation of *γ-crystallin* at 60 °C

Fig. 5 shows the kinetics of aggregation of γ-crystallin (γ-Cry) at 60 °C in the absence and in the presence of Wt, R69C and D109H αB-Crys. The initial kinetic data are represented in Table S4 in supplementary materials. Parameters I_{lim}, t^*, $t_{0.5}$ and m for lysozyme aggregation calculated using Eq. (5) are given in Table 1.

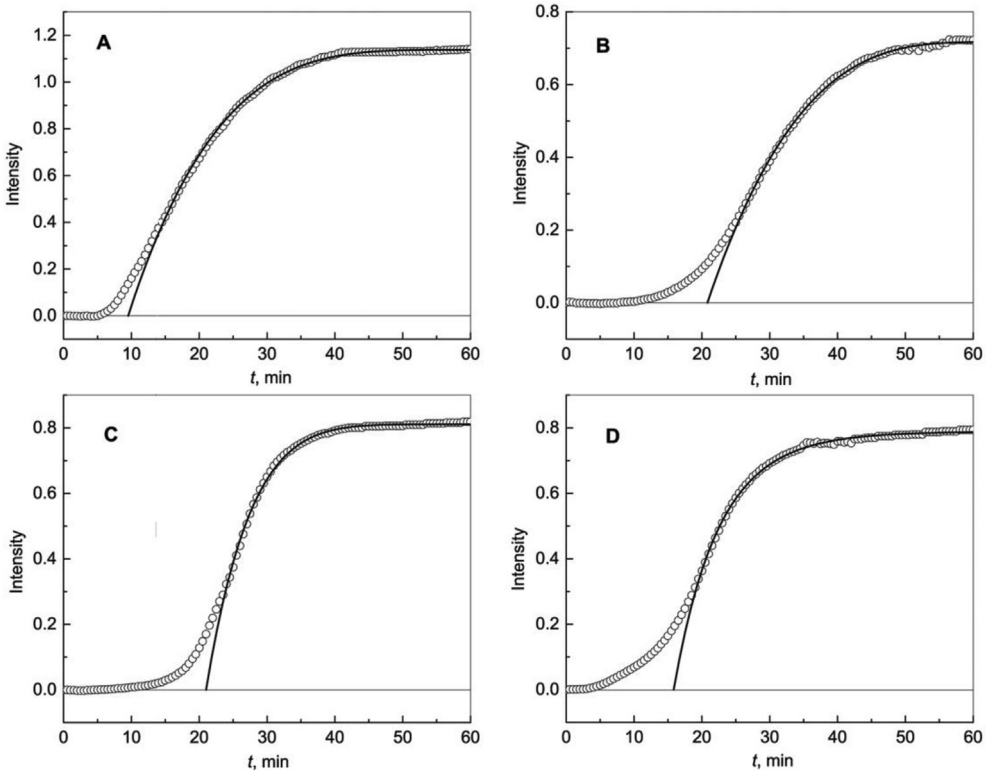

Fig. 5. Aggregation of γ-Cry (0.16 mg mL^{-1}) at 60 °C. (A) The dependence of the light scattering intensity (I) on time (t) for aggregation of γ-Cry in the absence of any additives. Points are experimental data. Solid curve was calculated from Eq. (5) at the following values of parameters: $I_{lim} = 1.138$, $t^* = 9.5$ min, $t_{0.5} = 8.0$ min and $m = 0.75$. (B) The dependence of I on t for aggregation of γ-Cry in the presence of Wt αB-Cry (0.08 mg mL^{-1}). Solid curve was calculated from Eq. (5) at the following values of parameters: $I_{lim} = 0.717$, $t^* = 20.8$ min, $t_{0.5} = 8.1$ min and $m = 0.69$. (C) The dependence of I on t for aggregation of γ-Cry in the presence of R69C mutant form of αB-Cry (0.08 mg mL^{-1}). Solid curve was calculated from Eq. (5) at the following values of parameters: $I_{lim} = 0.811$, $t^* = 21.0$ min, $t_{0.5} = 4.2$ min and $m = 0.85$. (D) The dependence of I on t for aggregation of γ-Cry in the presence of D109H mutant form of αB-Cry (0.08 mg mL^{-1}). Solid curve was calculated from Eq. (2) at the following values of parameters: $I_{lim} = 0.788$, $t^* = 15.8$ min, $t_{0.5} = 4.6$ min and $m = 1.03$.

2. Experimental design, materials, and methods

2.1. Chaperone-like activity assessment of R69C and D109H mutant αB-Crys

The chaperone-like activity of mutant αB-Crys was measured using different client proteins including insulin, lysozyme, catalase and γ-Cry [5]. Aggregation of bovine pancreatic insulin (0.3 mg mL^{-1}) and chicken egg white lysozyme (0.2 mg mL^{-1}) was induced with dithiothreitol (DTT; 20 mM) in buffer A at 40 °C. The heat-induced aggregation of γ-Cry and bovine liver catalase was performed at 60 °C. The molar ratio of chaperone/γ-Cry was set at 1:2. The aggregation of catalase (0.3 mg mL^{-1}) was induced in the presence of different chaperones. The light scattering of the client proteins was measured while the concentration of the chaperone was fixed at 0.1 mg mL^{-1}. The aggregation of γ-Cry was obtained in the presence of 0.08 mg mL^{-1} of Wt and mutant αB-Cry chaperones. The aggregation progress of the client proteins was monitored by measuring light scattering at 360 nm as a function of time, using a T90$^+$ UV–Vis spectrophotometer (PG Instrument Ltd., UK) equipped with a Peltier temperature controller. Moreover, all of the measurements were done in the absence of shaking/stirring condition.

Origin Pro 8.0 SR0 software was used for the calculations. To characterize the degree of agreement between experimental data and calculated values, we used the coefficient of determination R^2 (see Ref. [6]).

Funding

This work was supported by INSF (grant number 96008461), NIMAD (grant number 964854) and RSF (grant number 16-14-10055 to B.I.K.).

Acknowledgments

The authors appreciatively acknowledge the financial support of Shiraz University Research Council, Iran National Science Foundation, National Institute for Medical Research Development and the Russian Science Foundation.

Conflict of Interest

The authors declare that they have no known competing financial interests or personal relationships that could have appeared to influence the work reported in this paper.

Appendix A. Supplementary data

Supplementary data to this article can be found online at https://doi.org/10.1016/j.dib.2019.104922.

References

[1] M. Ghahramani, R. Yousefi, A. Krivandin, K. Muranov, B. Kurganov, A.A. Moosavi-Movahedi, Structural and functional characterization of D109H and R69C mutant versions of human αB-crystallin: the biochemical pathomechanism underlying cataract and myopathy development, Int. J. Biol. Macromol. S0141–8130 (2019) 34809–34813, https://doi.org/10.1016/j.ijbiomac.2019.09.239.
[2] B.I. Kurganov, Kinetics of protein aggregation. Quantitative estimation of the chaperone-like activity in test-systems based on suppression of protein aggregation, Biochemistry (Mosc.) 67 (2002) 409–422, https://doi.org/10.1023/a:1015277805345.
[3] K. Wang, B.I. Kurganov, Kinetics of heat- and acidification-induced aggregation of firefly luciferase, Biophys. Chem. 106 (2003) 97–109, https://doi.org/10.1016/s0301-4622(03)00134-0.
[4] B.I. Kurganov, Quantification of anti-aggregation activity of chaperones, Int. J. Biol. Macromol. 100 (2017) 104–117, https://doi.org/10.1016/j.ijbiomac.2016.07.066.
[5] K. Khoshaman, R. Yousefi, A.M. Tamaddon, S.S. Abolmaali, A. Oryan, A.A. Moosavi-Movahedi, B.I. Kurganov, The impact of different mutations at Arg54 on structure, chaperone-like activity and oligomerization state of human αA-crystallin: the pathomechanism underlying congenital cataract-causing mutations R54L, R54P and R54C, Biochim. Biophys. Acta Protein Proteonomics 1865 (2017) 604–618, https://doi.org/10.1016/j.bbapap.2017.02.003.
[6] Scientist for Experimental Data Fitting, Microsoft Windows Version 2.0, Micro-Math Inc, Salt Lake City, 1995.